  Bull. Chem. Soc. Jpn., 61, 1959—1965 (1988)

Coordination Selectivity in Aluminum(III) Complex with 8-Hydroxy-7-[(2-hydroxy-5-carboxyphenyl)azo]-5-quinolinesulfonic Acid: Evidence for Linkage Isomerism

Zhi-Ping Bai, Hisahiko Einaga,*,† and Jinsai Hidaka
Department of Chemistry, University of Tsukuba, Ibaraki 305
†Institute of Materials Science, University of Tsukuba, Ibaraki 305
(Received October 12, 1987)

The coordination reaction of 8-hydroxy-7-[(2-hydroxy-5-carboxyphenyl)azo]-5-quinolinesulfonic acid (hcqs) to aluminum(III) has been investigated spectrophotometrically in a weakly acidic aqueous solution (pH 2—5) with 0.1 mol dm^{-3} NaCl at 22.0 °C; the thermodynamic stability, kinetics, and mechanism of the formation of the aluminum(III) complex were deduced. The ligand rapidly coordinates to aluminum(III), with its 8-quinolinol (*O-N*) moiety, to form a yellow complex (metal : ligand=1 : 1), and then the complex slowly changes, via an intramolecular rearrangement, to a red complex with its dihydroxyazo (*O-N-O*) moiety, thus showing a linkage isomerism. In the first coordination process, the complex is formed mainly via a pathway of the reaction of $AlOH^{2+}$ with $Hhcqs^{3-}$. The coordination reaction mechanism of aluminum(III) with related ligands, 4-hydroxy-3-[(2-hydroxy-5-carboxyphenyl)azo]-1-naphthalenesulfonic and 7-[(4-carboxyphenyl)azo]-8-hydroxy-5-quinolinesulfonic acid, is also discussed.

The selectivity of coordination modes[1] in metal complexes is one of the fundamental functions of multidentate ligands because of their steric restrictions. In our previous papers,[1-4] the reactions of aluminum(III) with such multidentate ligands as 8-hydroxy-7-[(6-sulfo-2-naphthyl)azo]-5-quinolinesulfonic acid (nqs),[1,2] 7-[(3,6-disulfo-8-hydroxy-1-naphthyl)azo]-8-hydroxy-5-quinolinesulfonic acid (hns),[3] and 7-[(2-carboxyphenyl)azo]-8-hydroxy-5-quinolinesulfonic acid (pqs),[4] have been investigated. The selective coordination sites of these ligands were found to be the 8-quinolinol moiety for nqs, the dihydroxyazo moiety for hns, and the carboxyhydroxyazo moiety for pqs. These findings mean that the coordination ability of the azo nitrogen atom is lower than that of the quinoline nitrogen atom, but that the fused chelate ring structure facilitates the coordination of the azo nitrogen atom in the aluminum(III) complex. Furthermore, it has been found that these ligands react with aluminum(III) with a single rate-determining step to form mono-ligand complexes, which involve a five-membered chelate ring with the *O-N* coordination mode for nqs[1,2] and two six-membered fused chelate rings with the *O-N-O* coordination mode for hns[3] and pqs.[4]

In this work, 8-hydroxy-7-[(2-hydroxy-5-carboxyphenyl)azo]-5-quinolinesulfonic acid (hcqs, **1**), which potentially coordinates to aluminum(III) either with the dihydroxyazo (*O-N-O*) moiety to form five- and six-membered fused chelate rings or with the 8-quinolinol (*O-N*) moiety to form a five-membered chelate ring, was synthesized for the first time in order to investigate its coordination behavior to aluminum(III). It was found that hcqs initially reacts with aluminum(III) to form a yellow complex with the *O-N* coordination mode, but finally forms a red complex with the *O-N-O* mode; the complex shows a linkage isomerism. This paper will be concerned with a detailed investigation of the equilibrium, kinetics, and mechanism of the aluminum(III) complex with hcqs.

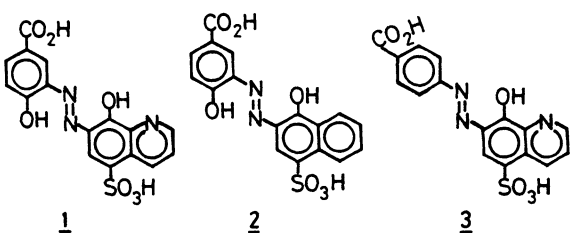

1 2 3

Experimental

Reagents. The ligand, hcqs, was synthesized by the diazotization of 3-amino-4-hydroxybenzoic acid and by coupling to 8-hydroxy-5-quinolinesulfonic acid in a conventional way. The crude product was purified by a repeated salting-out of the aqueous solution with NaCl at pH 7—8. Found: C, 31.77; H, 3.18; N, 6.80%. Calcd for $C_{16}H_{10}N_3O_7SNa \cdot 2NaCl \cdot 4.5H_2O$: C,31.54; H, 3.14; N, 6.90%.

In order to compare them, the ligands, 4-hydroxy-3-[(2-hydroxy-5-carboxyphenyl)azo]-1-naphthalenesulfonic acid (hcns, **2**) and 7-[(4-carboxyphenyl)azo]-8-hydroxy-5-quinolinesulfonic acid (cqs, **3**), were synthesized by the diazotization of 3-amino-4-hydroxybenzoic acid and coupling to 1-naphthol-4-sulfonic acid, and by the diazotization of 4-aminobenzoic acid and coupling to 8-hydroxy-5-quinolinesulfonic acid, respectively. These ligands were then purified by repeated precipitations from an alkaline aqueous solution by means of acidification with HCl. Found: C, 38.44; H, 3.68; N, 5.34%. Calcd for $C_{17}H_{11}N_2O_7SNa \cdot NaCl \cdot 3.5H_2O$: C,38.38; H, 3.41; N, 5.27%. Found: C, 43.89; H, 3.43; N, 9.54%. Calcd for $C_{16}H_{10}N_3O_6SNa \cdot 2.5H_2O$: C,43.64; H, 3.43; N, 9.54%.

An aqueous aluminum(III) solution was prepared by precipitating $Al(OH)_3$ from an aqueous solution of $AlK(SO_4)_2 \cdot 12H_2O$ with alkali, after which the hydroxide was dissolved in water with a minimum amount of HCl. The solution was acidified slightly to prevent the hydrolysis of

aluminum(III) ions. It was then standardized by the EDTA titration method. All the other chemicals used were of an analytical or equivalent grade.

Measurements. Electronic absorption spectral measurements were made on JASCO spectrophotometers, models UVIDEC-505 and -601C. The rapid kinetic measurements were done on a JASCO spectrophotometer, model SS-25, to which a stopped flow apparatus, model SFC-5, a data processor, model DP-500, and a RIKADENKI X-Y recorder, model RW-11, were attached. The slow kinetic runs were monitored on a JASCO spectrophotometer, model UVIDEC-1. All the kinetic runs were carried out in an aqueous solution of 0.1 mol dm^{-3} NaCl at 22.0±0.1 °C under pseudo-first-order kinetic conditions with respect to the aluminum(III) concentration (ligand concentration: (1—7)×10^{-5} mol dm^{-3}). The absorbance changes with time were followed at 495 nm for the aluminum(III) complex with hcqs, at 375 nm for that with hcns, and at 490 nm for that with cqs. The complex formation can be clearly recognized at these wavelengths, which correspond to the maxima or shoulders in the spectra of the ligands. The observed rate constant, k_{obsd}, was calculated from the slope of the linear relation $-\ln(A_i-A_f)$ vs. t on the basis of Eq. 1:

$$\ln[(A_i-A_f)/(A_t-A_f)]=k_{obsd}\cdot t \quad (1)$$

where A_i, A_t, and A_f stand for the absorbances at the initial state, at time t, and at the equilibrium state of the kinetic process respectively. The $k_{obsd(1)}$ and $k_{obsd(2)}$ values for the first and second steps in the case of hcqs were calculated separately on the basis of Eq. 1, because the two steps take place according to different time scales. The A_t vs. t data were separately simulated on an NEC personal computer, model PC-9801E.

The pH value, pH_{meas}, was measured with a HORIBA pH meter, model F7-SS, equipped with glass and 3.33 mol dm^{-3} KCl calomel electrodes. The hydrogen ion concentration, $-\log[H^+]$, was calculated from pH_{meas} according to Eq. 2:

$$-\log[H^+]=pH_{meas}+\log f_{H^+} \quad (2)$$

The activity coefficient of the hydrogen ion, f_{H^+} (0.923), was estimated by defining a solution containing 0.0100 mol dm^{-3} HCl and 0.0900 mol dm^{-3} NaCl at 22 °C as $-\log[H^+]\equiv 2.00$. An acetic acid-sodium acetate buffer solution of less than 0.01 mol dm^{-3} was used to adjust the hydrogen ion concentration.

Results

Electronic Absorption Spectra. Figures 1 and 2 show the absorption spectra of hcqs and its aluminum-(III) complexes, together with those of aluminum(III) complexes of hcns and cqs for comparison. The fully deprotonated species, hcqs^{4-}, gives its dominant peaks corresponding to $\pi^*\leftarrow\pi$ transitions in the 20.0×10^3 cm^{-1} region due to the azo group and at 33.0×10^3 cm^{-1} due to the quinoline and benzene rings. The same spectral features were observed in cqs^{3-} and hcns^{4-}. Protonations at the coordination sites in hcqs^{4-} cause characteristic spectral shifts, which were used for the estimation of the protonation constants.

In the hcqs-aluminum(III) system, the absorbance at 495 nm, which corresponds to an absorption maximum wavelength of H_2hcqs^{2-} (at pH 4.5), decreased rapidly to attain a constant value within 10 s; afterwards, the absorbance began to increase slowly with the time to reach a limiting value after 10 min. The rate of the slow process was independent of the aluminum(III) concentration. Curve (1) in Fig. 2 shows the absorption spectrum when the absorbance at 495 nm is at its minimum. Upon standing, the absorption spectrum changes gradually with the time to Curve (2), but thereafter it does not change. Figure 3 depicts the absorption spectral change with the time in the slow process. The four isosbestic points at 457, 357, 323, and 292 nm indicate that the yellow complex corresponding to Curve (1) changes quantitatively to the red complex corresponding to Curve (2) in Fig. 2. Furthermore, Fig. 2 clearly demonstrates that Curve (1) conforms well to the absorption spectrum (Curve(3)) of the aluminum(III) complex with cqs, which coordi-

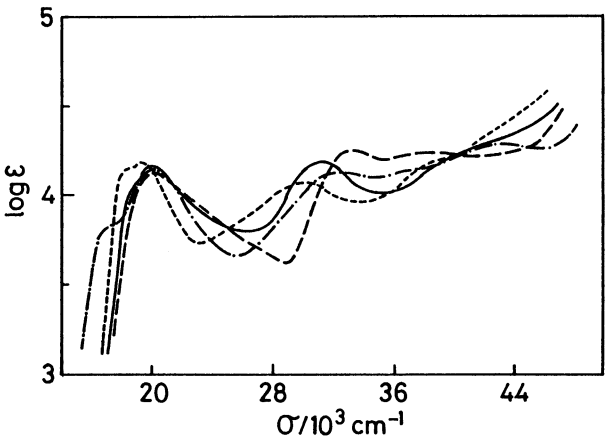

Fig. 1. Absorption spectra of hcqs: (----), H_3hcqs^- (pH 2.4); (——), H_2hcqs^{2-} (pH 5.0); (-·-·-), $Hhcqs^{3-}$ (pH 8.0); and (———), $hcqs^{4-}$ (pH 12.0). 0.1 mol dm^{-3} NaCl, 22 °C (cf. Table 1).

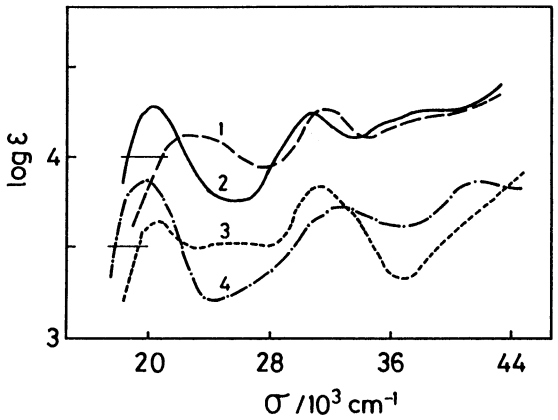

Fig. 2. Absorption spectra of aluminum(III) complexes with hcqs, hcns, and cqs at pH 4.5: 1, (———), Al(Hhcqs-*O*,*N*); 2, (——), Al(hcqs-*O*,*N*,*O*)$^-$; 3, (----), Al(cqs)$^-$; and 4, (-·-·-), Al(hcns)$^-$. Curves 3 and 4 are shifted 0.5 unit downward for clarity. 0.1 mol dm^{-3} NaCl, 22 °C.

nates solely with the 8-quinolinol moiety, and that Curve (2) conforms well to that (Curve(4)) of the aluminum(III) complex with hcns, which coordinates solely with the dihydroxyazo moiety.

Hence, it can be inferred that hcqs rapidly coordinates to aluminum(III) to give the yellow complex as a bidentate ligand with the *O-N* moiety and that it then rearranges to the red complex as a terdentate ligand with the *O-N-O* moiety:

$$\underset{\text{red}}{H_2\text{hcqs}^{2-}} + Al^{3+} \xrightarrow[\text{fast}]{k_{\text{obsd}(1)}} \underset{\text{yellow}}{\text{Al(Hhcqs-}O,N\text{)}} \xrightarrow[\text{slow}]{k_{\text{obsd}(2)}} \underset{\text{red}}{\text{Al(hcqs-}O,N,O\text{)}^-}$$

Protonations of Ligands and Stabilities of Complexes

Protonation. The protonation constants, K_{ai} (i= 1—4), of hcqs:

$$K_{ai}=[H_i\text{hcqs}^{(4-i)-}]/[H_{i-1}\text{hcqs}^{(5-i)-}][H^+] \quad (3)$$

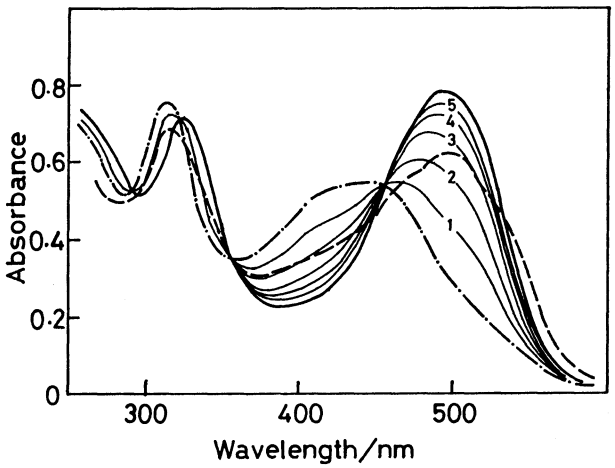

Fig. 3. Absorption spectral change with time of aluminum(III) complex with hcqs. (———), $H_2\text{hcqs}^{2-}$; (-·-·-), spectrum corresponding to yellow complex; (——), spectrum corresponding to red complex; (——), intermediate spectra from yellow to red complex recorded at 1, 1.5 min; 2, 3.5 min; 3, 6 min; 4, 9 min; and 5, 12 min. C_{Al}, 4.7×10^{-4} mol dm^{-3}; C_{hcqs}, 2.16×10^{-5} mol dm^{-3}, pH 4.5, 0.1 mol dm^{-3} NaCl, 22 °C.

were determined spectrophotometrically[4] with the aid of Eq. 4:

$$\log\{(A_{(i-1)\text{hcqs}}-A\text{x})/(A\text{x}-A_{(i)\text{hcqs}})\} = \log K_{ai}+\log[H^+] \quad (4)$$

where $A_{(i-1)\text{hcqs}}$, $A_{(i)\text{hcqs}}$, and $A\text{x}$ refer to the absorbances of solutions containing the ligand species $H_{i-1}\text{hcqs}^{(5-i)-}$ alone, $H_i\text{hcqs}^{(4-i)-}$ alone, and both of them respectively. Absorbance measurements were made at the following wavelengths: hcqs, 585, 345, and 295 nm (K_{a1}), 585 nm (K_{a2}), 550 and 360 nm (K_{a3}), and 360 nm (K_{a4}); hcns, 580 and 335 nm (K_{a1}), 508 and 265 nm (K_{a2}), and 527 nm (K_{a3}); cqs, 525 and 435 nm (K_{a1}), 530 nm (K_{a2}), and 510 nm (K_{a3}). The protonation constants of hcqs, together with those of hcns and cqs, are summarized in Table 1. A mutual comparison of these protonation constants and a comparison with those of the related ligands[1-4] indicate that, in the case of hcqs, K_{a1} corresponds to the protonation at the phenolate oxygen; K_{a2}, to that at the quinolinolate oxygen; K_{a3}, to that at the heterocyclic nitrogen; and K_{a4}, to that at the carboxylate oxygen atoms.

The compositions of the hcqs complexes were estimated by the method of continuous variation.[5] A sharp and single maximum at the ligand mole fraction of 0.5 was obtained for both the yellow and red complexes at 400, 497, and 270 nm, indicating that complexes with a 1 : 1 (Al : hcqs) composition are formed. The formation of the 1 : 1 complexes was also confirmed in the aluminum(III) complex with hcns (at 380 and 325 nm) and in that with cqs (at 519.5 and 320 nm).

Determination of Stability Constants. On the basis of the characteristic spectral features of the hcqs complexes, the protonation constants of hcqs, and the hydrolysis constant[6] of aluminum(III), $K_{OH}(=10^{-4.49}$ defined as $K_{OH}=[AlOH^{2+}][H^+]/[Al^{3+}]$), the 1 : 1 red complex formation equilibrium related to the $H_2\text{hcqs}^{2-}$ species at pH 2.69 can be defined as follows:

$$Al^{3+}+H_2\text{hcqs}^{2-} \rightleftharpoons \text{Al(hcqs)}^- + 2H^+ \quad (5)$$

The following materials balance relations hold for the present system:

$$C_{Al}=[Al^{3+}]+[AlOH^{2+}]+[\text{Al(hcqs)}^-] \quad (6)$$

Table 1. Protonations of Ligands and Stabilities of Complexes (0.10 mol dm^{-3} NaCl, 22 °C)

Ligand	hcqs	hcns	cqs	Remark
I	10.26±0.04	10.84±0.06	—	Phenolate
II	6.36±0.05	6.74±0.05	7.40±0.08	Quinolinolate, naphtholate
III	2.98±0.05	—	2.43±0.05	Quinoline
IV	3.60±0.10	4.25±0.05	2.90±0.05	Carboxylate
Complex	Al(hcqs-O,N,O)$^-$	Al(hcns)$^-$	Al(cqs)	
log β_{11}	14.15±0.10	15.27±0.10	7.49±0.10	

I) $\log(K_{a1}/\text{mol}^{-1}\text{ dm}^3)$ for hcqs, hcns; II) $\log(K_{a2}/\text{mol}^{-1}\text{ dm}^3)$ for hcqs, hcns, $\log(K_{a1}/\text{mol}^{-1}\text{ dm}^3)$ for cqs; III) $\log(K_{a3}/\text{mol}^{-1}\text{ dm}^3)$ for hcqs, $\log(K_{a2}/\text{mol}^{-1}\text{ dm}^3)$ for cqs; IV) $\log(K_{a4}/\text{mol}^{-1}\text{ dm}^3)$ for hcqs, $\log(K_{a3}/\text{mol}^{-1}\text{ dm}^3)$ for hcns, cqs.

$$C_{hcqs}=[H_2hcqs^{2-}]+[Hhcqs^{3-}]+[hcqs^{4-}]+[Al(hcqs)^-] \quad (7)$$

Equation 8 can be derived thus from Eqs. 5—7:

$$\log \alpha/r(1-\alpha)=\log \beta_{11}-\log K_{a1}K_{a2}-2\log[H^+]+\log[Al^{3+}] \quad (8)$$

$$\alpha\equiv[Al(hcqs)^-]/C_{hcqs}$$
$$r\equiv K_{a1}K_{a2}[H^+]^2/(1+K_{a1}[H^+]+K_{a1}K_{a2}[H^+]^2)$$
$$[Al^{3+}]\equiv(C_{Al}-\alpha C_{hcqs})/(1+K_{OH}/[H^+])$$

The experimental data are given in Fig. 4; the plot of $\log \alpha/r(1-\alpha)$ vs. $\log[Al^{3+}]$ is linear, with a unit slope. The $\log \beta_{11}$ ($\beta_{11}=[Al(hcqs)^-]/[Al^{3+}][hcqs^{4-}]$) value was determined to be 14.15±0.10 from the intercept; the stability constants are shown in Table 1.

Likewise, the 1 : 1 complex formation equilibrium related to $Hcqs^{2-}$ at pH 3.56 and to H_2hcns^{2-} at pH 2.83 can be defined as follows:

$$Al^{3+}+Hcqs^{2-} \rightleftharpoons Al(cqs)^-+H^+ \quad (9)$$

$$Al^{3+}+H_2hcns^{2-} \rightleftharpoons Al(hcns)^-+2H^+ \quad (10)$$

For cqs:

$$\log \alpha/r(1-\alpha)=\log \beta_{11}-\log K_{a1}-\log[H^+]+\log[Al^{3+}] \quad (11)$$

$$r\equiv K_{a1}[H^+]/(1+K_{a1}[H^+]+K_{a1}K_{a2}[H^+]^2)$$

For hcns:

$$\log \alpha/r(1-\alpha)=\log \beta_{11}-\log K_{a1}K_{a2}-2\log[H^+]+\log[Al^{3+}] \quad (12)$$

$$r\equiv K_{a1}K_{a2}[H^+]^2/(1+K_{a1}[H^+]+K_{a1}K_{a2}[H^+]^2)$$

The experimental data are plotted in Fig. 4 to obtain a $\log \beta_{11}$ value of 7.49±0.12 for the 1 : 1 cqs complex and a $\log \beta_{11}$ value of 15.27±0.10 for the 1 : 1 hcns complex; the stability constants are shown in Table 1.

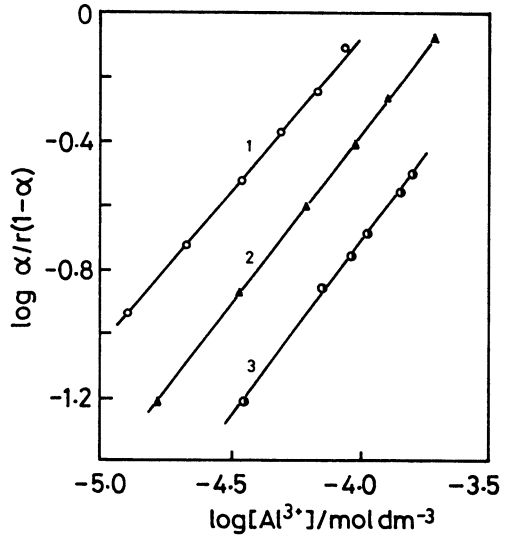

Fig. 4. Relations between $\log \alpha/r(1-\alpha)$ and $\log[Al^{3+}]$. 0.1 mol dm^{-3} NaCl, 22 °C. 1, for 1:1 hcqs complex(red), pH 2.69 (formate buffer), at 550 nm; 2, for 1:1 cqs complex, pH 3.56 (acetate buffer), at 405 nm; and 3, for 1:1 hcns complex, pH 2.83 (formate buffer), at 520 nm.

Kinetics and Mechanism. The formation of the hcqs complex can be treated in term of two consecutive reactions with different time scales: The rapid coordination of hcqs to aluminum(III) to form the yellow complex, Al(Hhcqs-*O,N*), followed by a slow intramolecular change to the red complex, $Al(hcqs\text{-}O,N,O)^-$. Each reaction step obeyed the first-order kinetics. A linear relation was obtained between the logarithmic absorbance change with time for more than 3.5 half-life periods for each step at 495 nm.

Rapid Process. By taking into consideration[7] the protonation constants of hcqs, the hydrolysis constant of aluminum(III), the stability constant of the 1 : 1 complexes, and the more rapid attainment of equilibria for the protolytic process[8] as compared with the complex formation process, which proceeds at pH 2—5, the rapid formation of Al(Hhcqs-*O,N*) can be considered to proceed as is shown in Scheme 1. Six possible

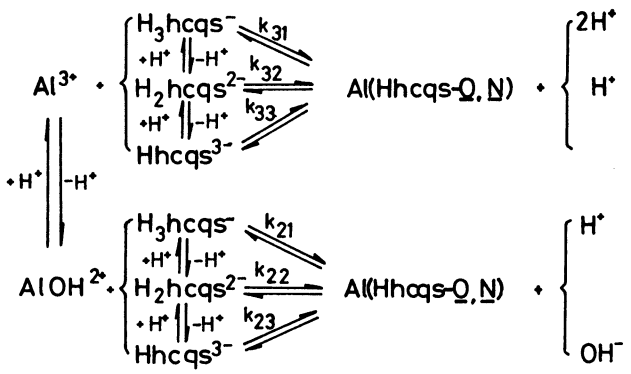

Scheme 1.

reaction pathways are proposed here, with their rate equations:

$$d[Al(Hhcqs\text{-}O,N)]/dt=\{k_{31}[H_3hcqs^-]+k_{32}[H_2hcqs^{2-}]+k_{33}[Hhcqs^{3-}]\}[Al^{3+}]+\{k_{21}[H_3hcqs^-]+k_{22}[H_2hcqs^{2-}]+k_{23}[Hhcqs^{3-}]\}[Al\,OH^{2+}]-\{k_{-31}[H^+]^2+(k_{-32}+k_{-21})[H^+]+(k_{-33}+k_{-22})+k_{-23}[OH^-]\}[Al(Hhcqs\text{-}O,N)] \quad (13)$$

Here, k_{ij} refers to the rate constant for the forward reaction pathway of $AlOH_{3-i}^{i+}$ (i=2 and 3) with $H_{4-j}hcqs^{j-}$, while k_{-ij} refers to the rate constant for the corresponding backward reaction pathway. Under the pseudo-first-order kinetic conditions with respect to the aluminum(III) concentration, the relation 14 between the modified rate constant, $k'_{obsd(1)}$, which can be defined by Eq. 15 from the $k_{obsd(1)}$ determined experimentally by using Eq. 1, while $[H^+]$ can be derived thus from Eq. 13:

$$k'_{obsd(1)}=k_{31}K_{a3}K_{a2}[H^+]^2+(k_{32}+k_{21}K_{a3}K_{OH})K_{a2}[H^+]+(k_{33}+k_{22}K_{a2}K_{OH})+k_{23}K_{OH}[H^+]^{-1} \quad (14)$$

Table 2. Kinetic Parameters (0.10 mol dm^{-3} NaCl, 22 °C)

Pathway	Rate constant/mol^{-1} dm^3 s^{-1}	Remark
$AlOH^{2+}+Hhcqs^{3-}$ (k_{23})	k_{23}: (1.37±0.35)×10^5	First step
Al(hcqs-*O*,*N*)(OH)→	k_{IV}: (3.43±0.45)×10^3	k_{IV}/s^{-1}, second step
$Al^{3+}+cqs^{3-}$(k_{33}) and $AlOH^{2+}+Hcqs^{2-}$(k_{22})	$k_{33}+k_{22}K_{a1}K_{OH}$: (1.34±0.40)×10^5	$K_{a1}=K_{a1(cqs)}$
$AlOH^{2+}+cqs^{3-}$(k_{23})	k_{23}: (7.20±0.30)×10^5	$K_{OH}=K_{OH(Al)}$
$Al^{3+}+Hhcns^{3-}$(k_{33}) and $AlOH^{2+}+H_2hcns^{2-}$(k_{22})	$k_{33}+k_{22}K_{a2}K_{OH}$: (4.44±0.46)×10^2	$K_{a2}=K_{a2(hcns)}$
$AlOH^{2+}+Hhcns^{3-}$(k_{23})	k_{23}: (3.91±0.35)×10^3	

$$k'_{obsd(1)} \equiv k_{obsd(1)}/\{1/\beta'_{11} + C_{Al}/[(K_{a3}K_{a2}[H^+]^2 + K_{a2}[H^+]+1)(1+K_{OH}/[H^+])]\} \quad (15)$$

where C_{Al} refers to the total concentration of aluminum(III) and β'_{11}, to the stability constant of Al(Hhcqs-*O*,*N*), which was tentatively estimated to be the same as that of Al(cqs). Figure 5 shows the experimental data plotted on the relation of $k'_{obsd(1)}$ vs. $[H^+]$; a linear relation with an intercept of zero, which indicates that Al(Hhcqs-*O*,*N*) is formed through the reaction pathway of $AlOH^{2+}$ with $Hhcqs^{3-}$. The rate constant, k_{23}, is given in Table 2.

Slow Process. In the slow process, the observed rate constant, $k_{obsd(2)}$, does not depend on C_{Al} at a constant hydrogen ion concentration; this is in contrast to the rapid process, in which $k_{obsd(1)}$ is linearly dependent on C_{Al}. This fact indicates that the slow process (the second reaction step) corresponds to an intramolecular rearrangement of the hcqs complex between two possible coordination modes of the ligand.

Scheme 2 shows the equilibria among possible complex species of Al(Hhcqs-*O*,*N*). Hence, the formation of the red complex, Al(hcqs-*O*,*N*,*O*)$^-$, can be expected via four possible reaction pathways, with the rate equations given as follows:

$$\begin{aligned} &d[Al(hcqs\text{-}O,N,O)]/dt \\ &\quad = -d[Al(Hhcqs\text{-}O,N)]/dt \\ &\quad = k_I[I] + k_{II}[II] + k_{III}[III] + k_{IV}[IV] \\ &\quad -\{k_{-I}[H^+] + (k_{-II}+k_{-III}) \\ &\quad + k_{-IV}[OH^-]\}[Al(hcqs\text{-}O,N,O)] \end{aligned} \quad (16)$$

By defining the modified rate constant, $k'_{obsd(2)}$, which can be defined by the use of Eq. 17 from the $k_{obsd(2)}$ value determined experimentally by using Eq. 1:

$$k'_{obsd(2)} \equiv k_{obsd(2)}/\{1/\beta''_{11} + 1/[(1+K_{a1}[H^+])(1+K_{OH}/[H^+])]\} \quad (17)$$

Eq. 18 can then be derived:

$$k'_{obsd(2)} = k_I K_{a1}^{II}[H^+] + (k_{II} + k_{III}K_{a1}^{IV}K_{OH}^{I}) + k_{IV}K_{OH}^{I}[H^+]^{-1} \quad (18)$$

Here, k_I, k_{II}, k_{III}, and k_{IV} are the rate constants for the forward pathways of the second reaction step related to the complex species of I, II, III, and IV; k_{-I}, k_{-II}, k_{-III}, and k_{-IV} are those for the reverse pathways corresponding to each species; β''_{11} is the stability constant of Al(hcqs-*O*,*N*,*O*)$^-$ with reference to Al(Hhcqs-*O*,*N*,); K_{a1}^{II} and K_{a1}^{IV} are the protonation constants of the complex species II and IV corresponding to the K_{a1} values of hcqs, and K_{OH}^{I} and K_{OH}^{II} are the hydrolysis constants of aluminum(III) in the complex species I and II respectively. In the following treatments, for convenience, K_{a1}^{II} and K_{a1}^{IV} were approximated to K_{a1}, and K_{OH}^{I} and K_{OH}^{II}, to K_{OH}. Figure 5 shows a linear relation with a zero intercept between $k'_{obsd(2)}$ and $[H^+]^{-1}$. That is, the intramolecular rearrangement

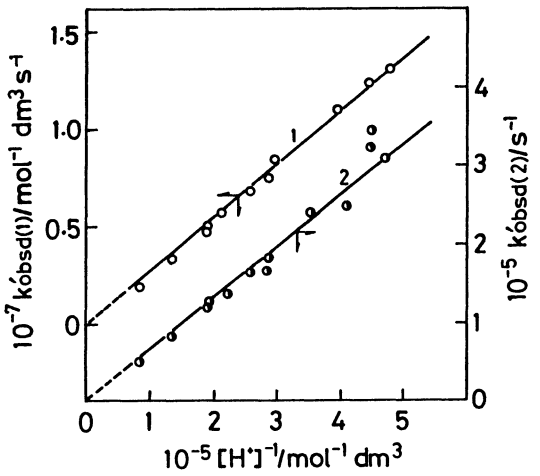

Fig. 5. Relation between $k'_{obsd(1)}$ and $1/[H^+]$ in the first step (1), and between $k'_{obsd(2)}$ and $1/[H^+]$ in the second step (2): C_{Al}, 4.7×10^{-4} mol dm^{-3}; C_{hcqs}, 2.16×10^{-5} mol dm^{-3}; 0.1 mol dm^{-3} NaCl, 22 °C; absorbance at 495 nm.

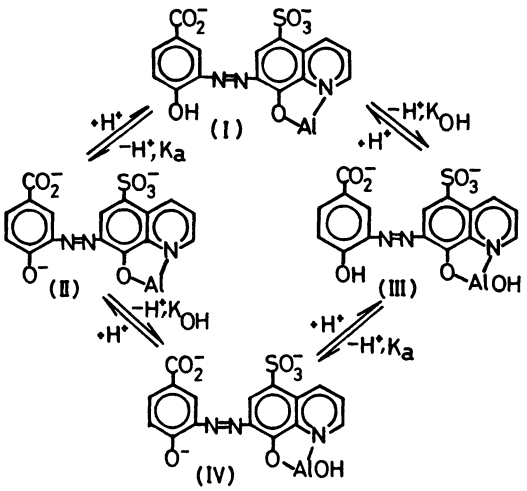

Scheme 2.

takes place through the pathway of the complex species IV. The rate constant, k_{IV}, is given in Table 2.

Formation of the cqs and the hcns Complexes. The kinetics of the formation of aluminum(III) complexes with cqs and hcns were also studied under pseudo-first-order kinetic conditions with respect to the aluminum-(III) concentration. The coordination reaction of cqs to aluminum(III) was rapid, just as in the case of the first step of that of hcqs to aluminum(III); a linear relation was found between the logarithmic absorbance change with time for more than 3.5 half-life periods at 316, 400, and 495 nm. On the contrary, the coordination reaction of hcns to aluminum(III) was rather slow as compared with that of cqs, and the reaction rate was of the same order as that of the second step of the hcqs complex; a linear relation was obtained between the logarithmic absorbance change with time for more than 3.5 half-life periods at 495 nm.

The same mathematical treatments as in the case of the rapid process of the hcqs complex were carried out for the cqs and the hcns complexes in order to deduce the reaction pathways; similar relations between the modefied rate constant, k'_{obsd}, and $[H^+]$ were derived as follows:

For the cqs complex:

$$K'_{obsd} = k_{31}K_{a1}K_{a2}[H^+]^2 + (k_{32} + k_{21}K_{a2}K_{OH})K_{a1}[H^+] + (k_{33} + k_{22}K_{a1}K_{OH}) + k_{23}K_{OH}[H^+]^{-1} \quad (17)$$

For the hcns complex:

$$K'_{obsd} = k_{32}K_{a1}K_{a2}[H^+]^2 + (k_{33} + k_{22}K_{a2}K_{OH})K_{a1}[H^+] + (k_{34} + k_{23}K_{a1}K_{OH}) + k_{24}K_{OH}[H^+]^{-1} \quad (18)$$

Here, k_{ij} have the usual meanings. The plots of the experimental data in Fig. 6 indicate a linear relation between k'_{obsd} and $1/[H^+]$ for the cqs complex and a linear relation between k'_{obsd} and $[H^+]$ for the hcns complex. The kinetic parameters are summarized in Table 2.

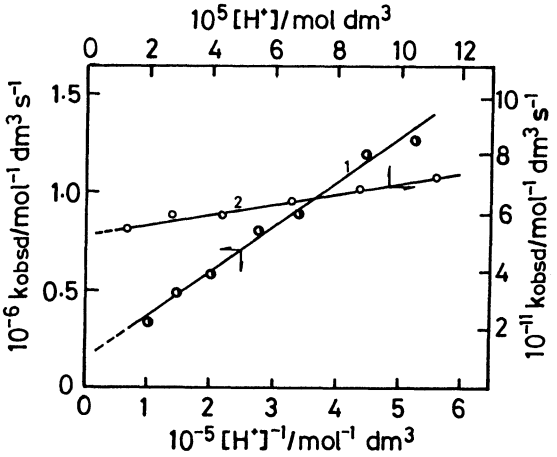

Fig. 6. Relation between k'_{obsd} and $1/[H^+]$ for 1:1 cqs complex at 490 nm (1); and between k'_{obsd} and $[H^+]$ for 1:1 hcns complex at 375, 330, and 265 nm (2). C_{Al}, 4.7×10^{-4} mol dm^{-3}; C_{cqs} or C_{hcns}, 2.4×10^{-5} mol dm^{-3}; 0.1 mol dm^{-3} NaCl, 22 °C.

Discussion

The ligand hcqs shows coordination behavior unique to aluminum(III); namely, it forms two types of complexes, Al(Hhcqs-*O,N*) (yellow) and Al(hcqs-*O,N,O*)$^-$ (red),[9] which are in the linkage isomerism. This is unlike hns and pqs, which coordinate selectively to aluminum(III) only with one of the two coordination modes, although the linkage isomerism is possible for hns and pqs as well as for hcqs. The molecular models of the ligand species suggest that hcqs is stabilized more to a *trans-O,O* form (phenolate and quinolinolate oxygen atoms) with regard to the azo group by the intramolecular hydrogen bonds, whereas hns is less stabilized to the *trans-O,O* form with the intramolecular hydrogen bonds, while pqs has no such hydrogen bonds for the stabilization of the *trans-O,O* form. Hence, it can tentatively be inferred that the hydroxyl group ortho to the azo group on the aromatic ring opposite the 8-quinolinol moiety is prerequisite for the linkage isomerism.

The ligand hcqs first coordinates to aluminum(III) with the 8-quinolinol moiety to form the yellow complex. The absorption spectral and kinetic evidence indicates that the coordination behavior of hcqs to aluminum(III) was superposable on that of cqs, which functions as the *O-N* bidentate ligand, but was quite different from that of hcns, which functions as the *O-N-O* terdentate ligand. Taking the differences in molecular structure of these ligands into consideration,[10] Table 2 clearly indicates that the rate constants for each of the reaction pathways of hcqs and of cqs are of the same magnitude as those for the corresponding pathways of hns, nqs, pqs, and hqs.[1-4] Therefore, the rate-determining steps of hcqs and cqs for their coordination to aluminum(III) must be the same as those of hns, nqs, pqs, and hqs; donation via the 8-quinolinolate oxygen atom to aluminum(III). Chelate ring closure as the rate-determining step can probably be ruled out because the rate constants for cqs, hcqs, nqs, and hqs, all having the *O-N* bidentate ring, are intrinsically of the same magnitude, and they agree with those of hns and pqs. Incidentally, the considerably small rate constant for hcns compared with the rate constants for hns and pqs indicates that the chelate ring closure is the rate-determining step in the coordination of hcns to aluminum(III). Hence, it is inferred that the formation of Al(Hhcqs-*O,N*) proceeds through the coordination of the 8-quinolinolate oxygen atom to aluminum(III) as the rate-determining step,[1-4] followed by a rapid chelate ring closure to form a five-membered chelate ring.

The formation of the red hcqs complex shows a unique kinetic feature: The rate constant for the formation of the red complex is considerably smaller than

that of the cqs complex; rather, it is in line with that of the hcns complex. The molecular models of hcqs and hcns indicate that the coordination of these ligands with the *O-N-O* terdentate moieties requires transformation from the *trans-O,O* to the *cis-O,O* form with regard to the azo group by breaking the intramolecular hydrogen bond(s) after the coordination through the 8-quinolinolate oxygen atom as unidentate ligands. The small rate constants for the formation of the red hcqs complex and of the hcns complex reflect some contribution of this transformation; therefore, it may be concluded that the linkage isomerization of the yellow hcqs complex to the red one and the formation of the hcns complex proceed with the chelate ring closure as the rate-determining step.

Finally, it should be noted that hcqs and the related ligands can be classified into two groups with respect to the experimental relation of the modified rate constant, k'_{obsd} vs. $[H^+]$; linear relations between k'_{obsd} and $[H^+]$ hold for hcns, hns, pqs, and hqs, whereas linear relations between k'_{obsd} and $[H^+]^{-1}$ hold for hcqs, cqs, and nqs. The classification can be explained in terms of the basicity (protonation constant) of the oxygen donor atom on the quinoline ring; those ligands having a higher basicity conform to the former relation, while those having a lower basicity conform to the latter relation. This evidence also supports the important role of the oxygen atom in the 8-quinolinol moiety on the reaction kinetics with aluminum(III), especially the rate-determining step, of hcqs and the related multidentate ligands.

References

1) K. Hayashi, K. Okamoto, J. Hidaka, and H. Einaga, *J. Chem. Soc., Dalton Trans.*, **1982**, 1377.

2) K. Hayashi, K. Okamoto, J. Hidaka, and H. Einaga, *J. Coord. Chem.*, **12**, 243 (1983).

3) H. Iwasaki, K. Okamoto, J. Hidaka, and H. Einaga, *J. Coord. Chem.*, **12**, 219 (1983).

4) I. Ohkura, K. Fujiwara, K. Okamoto, J. Hidaka, and H. Einaga, *J. Coord. Chem.*, **13**, 221 (1984).

5) H. L. Schläfer, "Komplexbilbung in Lösung," Springer, Berlin (1961), Chap. 8.

6) L. P. Holmes, D. L. Cole, and E. M. Eyring, *J. Phys. Chem.*, **72**, 301 (1968).

7) Y. Hara, K. Okamoto, J. Hidaka, and H. Einaga, *Bull. Chem. Soc. Jpn.*, **57**, 1211 (1984).

8) M. Eigen, *Pure Appl. Chem.*, **6**, 97 (1963).

9) In this type, hcqs is able to form two kinds of chelate ring arrangements, depending upon which nitrogen atom in the azo group serves as a donor atom. They can be considered to be in equilibrium because of the high lability of the aluminum(III) complex and the lack of any difference in steric restrictions between these arrangements.

10) There are several pairs of reaction pathways proceeding in a parallel way and indistinguishable by a kinetic investigation because of proton ambiguity. The highest probable rate constant for each reaction pathway was tentatively estimated for the discussion.